Rigid band model for prediction of magnetostriction of iron-gallium alloys

Y. N. Zhang, J. X. Cao, and R. Q. Wu[a)]
Department of Physics and Astronomy, University of California, Irvine, California 92697, USA

(Received 10 December 2009; accepted 23 January 2010; published online 11 February 2010)

Using the highly precise full potential linearized augmented plane wave method, we determined atomic structure and the magnetostriction of $Fe_{100-x}Ga_x$ with $x<19\%$. It is demonstrated that the extraordinary enhancement of magnetostrictive coefficient of $Fe_{100-x}Ga_x$ at low concentration stems from intrinsic electronic origins. Moreover, we recognized the potential of using a rigid band model for the prediction of magnetostriction of intermetallic alloys, through studies of ternary alloys with Zn substitution into $Fe_{87.5}Ga_{12.5}$. © *2010 American Institute of Physics*. [doi:10.1063/1.3318420]

It is striking that the tetragonal magnetostrictive coefficient (λ_{001}) of $Fe_{100-x}Ga_x$ alloys (Galfenol) increases monotonically with the concentration of Ga till $x=18-20$ to as large as 400 ppm.[1–6] This offers great opportunities for various applications such as MEMS, sensors, and transducers, and has inspired extensive interdisciplinary activities to search for better magnetostrictive materials.[7–9] However, advance in this direction is very limited so far, owing to the absence of predictive theoretical models for the description of magnetostriction in intermetallic alloys. Extrinsic origins including the field-induced rotation of DO_3-DO_{22} nanoprecipitates have been proposed to explain the extraordinary enhancement of magnetostriction in Galfenol.[10,11] However, the relevance of this model remains doubtful since most single crystalline samples have no obvious phase mixture.[12,13] On the other hand, recent density functional calculations for homogeneous $Fe_{100-x}Be_x$ and $Fe_{100-x}Ge_x$ alloys correctly reproduced the $\lambda_{001}(x)$ curves,[14–16] indicating that the magnetostriction in these materials should be governed by intrinsic electronic factors. Furthermore, it was recognized that magnitude and sign of λ_{001} of Galfenol strongly depends on the local arrangements of minority atoms at high concentration.[17] The presence of B_2-like Ga–Ga pairs was reported by several groups,[18,19] and was assigned as the main reason for the enhancement of magnetostriction in Galfenol.[20] Obviously, more systematic theoretical studies are needed to resolve puzzles in this field.

In this letter, we demonstrate the validity and predictive capability of density functional calculations for the studies of magnetostriction in binary and ternary $Fe_{100-x}Ga_x$ alloys. It is clearly shown that the enhancement of λ_{001} in Galfenol with small x (<19) stems from intrinsic electronic origins. Furthermore, we found that the trend of λ_{001} can be predicted through a rigid band approach, using $Fe_{87.5}Ga_{12.5}$, $Fe_{87.5}Ga_{6.75}Zn_{6.75}$ and $Fe_{87.5}Zn_{12.5}$ as model systems. Our findings provide guidance for the manipulation of magnetostriction in Galfenol, by replacing Ga with Zn or other metalloid elements.

We used the full potential linearized augmented plane wave methods[21] to solve the density functional Kohn–Sham equations. The spin-polarized generalized gradient approximation was adopted for the description of exchange-correlation interactions among electrons.[22] No shape approximation was assumed for charge, potential, and wave function expansions. The core electrons were treated fully relativistically, while the spin-orbit coupling term was invoked second variationally for the valence states.[23] Energy cutoffs of 225 Ry and 16 Ry were chosen for the charge-potential and basis expansions in the interstitial region, respectively. In the muffin-tin region ($r_{Fe}=1.11$ Å and $r_{Ga}=1.22$ Å), charge, potential, and basic functions were expanded in terms of spherical harmonics with a maximum angular momentum of $l_{max}=8$. The convergence of electronic and magnetic properties against the choice of number of k-points and wave function expansion were carefully monitored. The self-consistence was assumed when the root-mean-square differences between the input and output charges and spin densities are less than 1.0×10^{-4} $e/(\text{a.u.})^3$. To avoid the complexity of nonuniform distribution of metalloid atoms and local precipitation, we focused on the intrinsic electronic effects on the enhancement of λ_{001} in systems with $x<19$.

We placed iron and metalloid atoms in the bcc lattice, with a 16-atom or 54-atom supercell. The lattice sizes and atomic positions were optimized according to the energy minimization procedures guided by atomic forces. For cases with $x=12.5$ and $x=18.75$ that have two and three metalloid atoms in the 16-atom unit cell, we investigated all nonequivalent distribution patterns and calculated their magnetostrictive coefficients with the most preferential configurations. As discussed before,[23,24] λ_{001} can be determined from the strain (ε) dependences of magnetocrystalline anisotropy energy (E_{MCA}) and total energy (E_{tot}) as

$$\lambda_{001}=\frac{2}{3}\frac{dE_{MCA}/d\varepsilon}{d^2E_{tot}/d\varepsilon^2}. \quad (1)$$

We applied different tetragonal strains along the z-axis with the constant-volume distortion mode (i.e., $\varepsilon_x=\varepsilon_y=-\varepsilon/2$). For example, results of E_{MCA} and E_{tot} of $Fe_{87.5}Ga_{12.5}$ are presented in Fig. 1. Both E_{MCA} and E_{tot} are smooth functions of ε and permit reliable polynomial fittings, indicating the high precision of our theoretical data. The value of λ_{001} determined with the slope of E_{MCA} and the curvature of E_{tot} at $\varepsilon=0$ is 128 ppm for $Fe_{87.5}Ga_{12.5}$, a value that agrees excellently with experimental data.

Figure 2 displays the optimal geometries the corresponding λ_{001} of $Fe_{100-x}Ga_x$ alloys for $x=1.85$, 6.25, 12.5, and 18.75, along with the experimental data. Obviously, density functional calculations reproduce the experimental $\lambda_{001}(x)$ curve in the entire range of x explored here. This suggests

a)Electronic mail: wur@uci.edu.

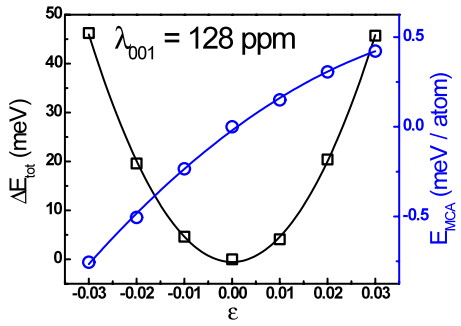

FIG. 1. (Color online) Calculated strain dependences of E_{tot} and E_{MCA} of $Fe_{87.5}Ga_{12.5}$.

that the monotonic increase in λ_{001} in this concentration range stems from intrinsic electronic origins, rather than from extrinsic factors such as precipitation. Experimentally, it was also reported that there is no link between the magnetic domains and the magnetostriction enhancement by Ga addition.[20] Furthermore, either slow cooled or rapidly quenched Galfenol samples with $x<17\%$ show almost identical magnetostriction.[7] Therefore, we may conclude that the magnetic field induced motions of precipitates (if there are any) or domain walls are insignificant for the phenomenal enhancement of magnetostriction of Galfenol, at least for samples with $x<19\%$. Nonetheless, deviation between theory and experimental data gradually become noticeable at the high-x end in Fig. 2 (to 14% or ~50 ppm at $x=18.75\%$). Therefore, the development of complex local structures is expected to play more important role afterwards. It is believed that the formation of ordered DO_3 structure leads to the large dip in the $\lambda_{001}(x)$ curve at $x\sim24$. The mechanism for the second peak in the $\lambda_{001}(x)$ curve at $x\sim28$ still remains mysterious. We found that the tetragonal shear modulus of Galfenol decreases almost linearly with x, to about 18–20 GPa at $x=18.75$. These results also agree with experimental data,[25] and suggest that the lattice softening is another important factor for the large enhancement of λ_{001} in these alloys.

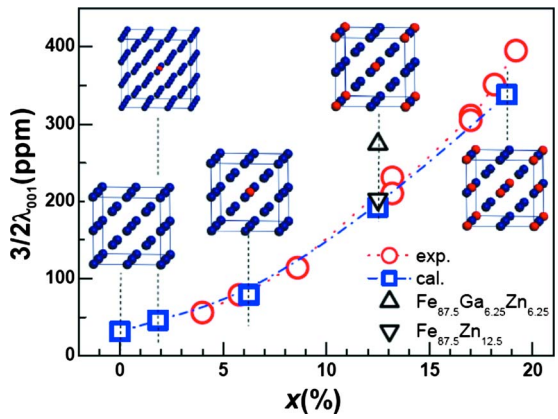

FIG. 2. (Color online) Tetragonal magnetostriction constant (3/2) λ_{001} as a function of the Ga composition. Circles are the experimental data taken at room temperature and squares are results from the present calculations at 0 K, respectively. Triangles show calculated results for $Fe_{87.5}Ga_{6.75}Zn_{6.75}$ and $Fe_{87.5}Zn_{12.5}$, with either one or both Ga being substituted by Zn in the unit cell. Insets are the atomic configurations used in the *ab initio* calculations. Blue/dark gray and red/light gray balls are for Fe and Ga atoms, respectively.

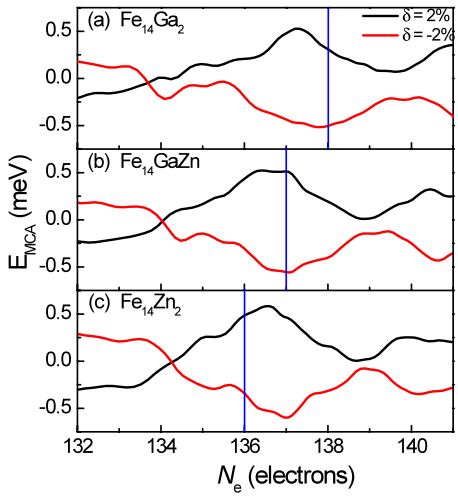

FIG. 3. (Color online) The calculated E_{MCA} against the band filling, N_e, for $Fe_{87.5}Ga_{12.5}$, $Fe_{87.5}Ga_{6.25}Zn_{6.25}$, and $Fe_{87.5}Zn_{12.5}$ with +2% and −2% lattice distortions along the z-axis.

Now we discuss the possibility of using the density functional approach along with rigid band model for prediction of magnetostriction in intermetallic alloys. To this end, the strain ($\varepsilon=\pm2\%$) induced magnetic anisotropy energies of $Fe_{87.5}Ga_{12.5}$ are given in Fig. 3(a) versus the number of electrons in the unit cell, N_e. Here, moving the position of the Fermi level over the fixed band structure changes values of N_e. Note that large E_{MCA} at the real Fermi level, denoted by the vertical solid lines in Fig. 3, corresponds to strong magnetostriction. It is clear that λ_{001} of $Fe_{87.5}Ga_{12.5}$ can be further enhanced by taking away about one electron from the unit cell, as shown in Fig. 3(a). Practically, this can be done through Zn substitution for Ga, assuming that Ga and Zn behave similarly toward the hybridization with their neighboring iron atoms.

To verify the applicability of this approach, we did self-consistent calculations for $Fe_{87.5}Ga_{6.25}Zn_{6.25}$ and $Fe_{87.5}Zn_{12.5}$, by replacing one or two Ga atoms with Zn. Interestingly, the three sets of $E_{MCA}(N_e)$ curves in Fig. 3 are very similar. The Fermi level of $Fe_{87.5}Ga_{6.25}Zn_{6.25}$ locates right at the peaks of the $E_{MCA}(N_e)$ curves in Fig. 3(b), which leads to $\lambda_{001}=183$ ppm, 43% larger than that of $Fe_{87.5}Ga_{12.5}$. Also as predicted according to the rigid band analysis, further reduction of N_e decreases λ_{001}, to 134 ppm for $Fe_{87.5}Zn_{12.5}$. Moreover, curves of density of states in Fig. 4 also indicate that substitution of Zn for Ga mainly causes band shift against the Fermi level but hardly changes the band structure. Therefore, the applicability of the rigid band model can be established for the prediction of magnetostriction of these alloys in a reasonable range of N_e. Synergistic experimental/theoretical studies along this direction are very promising for the design of excellent magnetostrictive materials. So far, experimental studies showed that most ternary additions such as Al, Cr, Co, and Ni typically result in reduction in magnetostrictive performance of Galfenol, except Sn.[7]

We found that Fe atoms nearest to Ga give the largest contributions to the magnetoelastic coupling, i.e., the strain dependence of E_{MCA}. Since the Fe–Ga hybridization is much weaker than that between Fe–Fe, the $d_{xz,yz}$ states become "dangling" bonds and shift in energy from the edges to the center of Fe 3*d*-band. As highlighted by the arrow in Fig. 4, Galfenol has high peaks right above E_F in the minority spin

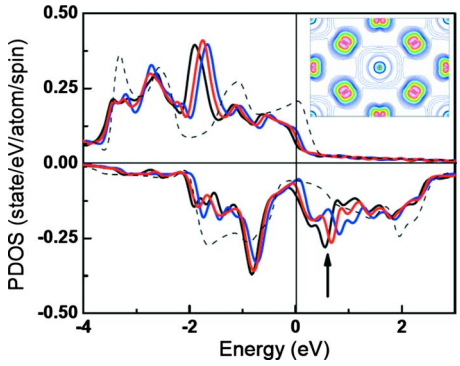

FIG. 4. (Color online) The projected density of states for $d_{xz,yz}$ orbitals of the Fe atoms nearest to Ga (or Zn) in $Fe_{87.5}Ga_{12.5}$ (black lines), $Fe_{87.5}Ga_{6.25}Zn_{6.25}$ (red/light gray lines), and $Fe_{87.5}Zn_{12.5}$ (blue/dark gray lines). The dash lines give the corresponding results for the bcc bulk Fe. Positive and negative regions are for the spin-up and spin-down parts, respectively. Zero energy indicates the position of the Fermi level. The arrow points out the nonbonding $d_{xz,yz}$ states, of which the wave functions are shown in the inset.

channel, in contrast to the valley at the same place for the pure bulk Fe. On the other hand, tetragonal lattice strain alters the energy position and occupation of e_g states. The strong spin-orbit coupling interaction between $d_{xz,yz}$ and e_g states across the Fermi level gives rise to the large magnetostriction.[23] For instance, the negative contribution of $\langle z^2|L_x|xz,yz\rangle$ to E_{MCA} under the tetragonal stretch was assigned as the main reason for the large negative magnetostriction in the $DO_3-Fe_{75}Ge_{25}$ alloy.[17] Obviously, changing N_e alters the occupation of states and thereby the leading pairs of states across the new Fermi level. To attain large magnetostriction, we want to capture the pair of states across E_F that are close in energy for strong spin-orbit coupling interaction.

In summary, high-quality density-functional calculations are reliable for the determination of λ_{001} of $Fe_{100-x}Ga_x$ alloys with $x<19\%$. Furthermore, we demonstrated the capability of using the rigid band model to predict magnetostrictive coefficients and explained the physical origin. Zn is proposed as a good substituent for Ga for the further enhancement of magnetostriction of $Fe_{87.5}Ga_{12.5}$, due to the change in the number of valence electrons. Density functional approach provides an excellent guideline.

The authors thank Dr. A. E. Clark, Dr. K. B. Hathaway, and Dr. M. Wun-Fogle for insightful discussions. Work was supported by the ONR (Grant No. N00014-08-1-0143) and the NSF (Grant No. DMR-0706503). Calculations were performed on the DOD supercomputers.

[1]A. E. Clark, J. B. Restorff, M. Wun-Fogle, T. A. Lograsso, and D. L. Schlagel, IEEE Trans. Magn. **36**, 3238 (2000).
[2]J. R. Cullen, A. E. Clark, M. Wun-Fogle, J. B. Restorff, and T. A. Lograsso, J. Magn. Magn. Mater. **226-230**, 948 (2001).
[3]A. E. Clark, K. B. Hathaway, M. Wun-Fogle, J. B. Restorff, T. A. Lograsso, V. M. Keppens, and G. Petculescu, J. Appl. Phys. **93**, 8621 (2003).
[4]R. A. Kellogg, A. B. Flatau, A. E. Clark, M. Wun-Fogle, and T. A. Lograsso, J. Appl. Phys. **91**, 7821 (2002).
[5]R. Q. Wu, Z. X. Yang, and J. S. Hong, J. Phys.: Condens. Matter **15**, S587 (2003).
[6]A. E. Clark, J. B. Restorff, M. Wun-Fogle, K. W. Dennis, T. A. Lograsso, and R. W. McCallum, J. Appl. Phys. **97**, 10M316 (2005).
[7]E. M. Summers, T. A. Lograsso, and M. Wun-Fogle, J. Mater. Sci. **42**, 9582 (2007).
[8]L. Dai, J. Cullen, M. Wuttig, T. A. Lograsso, and E. Quandt, J. Appl. Phys. **93**, 8627 (2003).
[9]A. E. Clark, J. B. Restorff, M. Wun-Fogle, K. B. Hathaway, T. A. Lograsso, M. Huang, and E. M. Summers, J. Appl. Phys. **101**, 09C507 (2007).
[10]S. Bhattacharyya, J. R. Jinschek, A. Khachaturyan, H. Cao, J. F. Li, and D. Viehland, Phys. Rev. B **77**, 104107 (2008).
[11]H. Cao, P. M. Gehring, C. P. Devreugd, J. A. Rodriguez-Rivera, J. Li, and D. Viehland, Phys. Rev. Lett. **102**, 127201 (2009).
[12]Q. Xing, Y. Du, R. J. McQueeney, and T. A. Lograsso, Acta Mater. **56**, 4536 (2008).
[13]M. Huang and T. A. Lograsso, Appl. Phys. Lett. **95**, 171907 (2009).
[14]G. Petculescu, J. B. LeBlanc, M. Wun-Fogle, J. B. Restorff, W. C. Burton, J. X. Cao, R. Q. Wu, W. M. Yuhasz, T. A. Lograsso, and A. E. Clark, IEEE Trans. Magn. **45**, 4149 (2009).
[15]S. C. Hong, W. S. Yun, and R. Q. Wu, Phys. Rev. B **79**, 054419 (2009).
[16]J. X. Cao, Y. N. Zhang, W. J. Ouyang, and R. Q. Wu, Phys. Rev. B **80**, 104414 (2009).
[17]R. Q. Wu, J. Appl. Phys. **91**, 7358 (2002).
[18]Q. Xing and T. A. Lograsso, Appl. Phys. Lett. **93**, 182501 (2008).
[19]S. Pascarelli, M. P. Ruffoni, R. Sato Turtelli, F. Kubel, and R. Grössinger, Phys. Rev. B **77**, 184406 (2008).
[20]J. Cullen, P. Zhao, and M. Wuttig, J. Appl. Phys. **101**, 123922 (2007).
[21]E. Wimmer, H. Krakauer, M. Weinert, and A. J. Freeman, Phys. Rev. B **24**, 864 (1981); M. Weinert, E. Wimmer, and A. J. Freeman, *ibid.* **26**, 4571 (1982).
[22]J. P. Perdew, Phys. Rev. B **33**, 8822 (1986); J. P. Perdew, K. Burke, and M. Ernzelhof, Phys. Rev. Lett. **77**, 3865 (1996).
[23]R. Q. Wu and A. J. Freeman, J. Magn. Magn. Mater. **200**, 498 (1999).
[24]X. D. Wang, R. Q. Wu, D. S. Wang, and A. J. Freeman, Phys. Rev. B **54**, 61 (1996).
[25]G. Petculescu, K. B. Hathaway, T. A. Lograsso, M. Wun-Fogle, and A. E. Clark, J. Appl. Phys. **97**, 10M315 (2005).